Electronic supplementary material (ESM)

ESM text: Methods

Skeletal muscle cell culture, transfection and plasmids. The techniques of muscle satellite cell isolation and growth have been described in detail previously, including the fact that the extent of differentiation into myotubes was similar in cells from healthy and type 2 diabetes participants [1,2]. Briefly, skeletal muscle cell cultures were established from muscle tissue obtained by needle biopsy samples of the vastus lateralis. Satellite cells were obtained by tryptic digestion of muscle biopsy material. Cells were propagated in culture in SkGM media (Lonza, Walkersville, MD), supplemented with the accompanying bullet kit but omitting insulin. At ~60% confluence cells were split into the required plates. Cells were used after the first passage. After attaining 80-90% confluence, cells were fused in a-MEM containing 2% fetal bovine serum (FBS), 1% penicillin/streptomycin. Mycoplasma-free myotubes were transfected on day 4 after fusion and the experiments were performed at day 5 and 6. Transfections were performed using Lipofectamine and Plus Reagent (Thermo Fisher Scientific, Waltham, MA, USA). No-codifying [1], IF1 [1] and mutant-IF1 (S39A, constitutively active; S39E, inactive; [2]) plasmids were used. Plasmid sequences are presented in earlier publications (10; 22). Suppression of IF1 expression was performed using a specific small interfering RNA (siRNA) (QIAGEN, Valencia, CA, USA, catalog # S100908075) at a final concentration of 20 nmol/l. An inefficient siRNA sequence, Silencer Select Negative Control #1 (Thermo Fisher Scientific), was used as a control. Where indicated, cells were treated with carnitine (1 mmol/l); etomoxir (100 μmol/l), the H^+-ATP synthase inhibitor oligomycin (OL, 5 μmol/l); the PKA agonist dbcAMP (100 μmol/l) or competitive PKA inhibitor H89 (10 μmol/l) for the indicated times before processing. Different experimental groups were treated and assessed simultaneously for each

experiment. Media and muscle myotubes were used for experiments or lysed in extraction buffer (see Buffer Composition) and stored at -80°C until analyzed.

Determination of the activity of OXPHOS complexes. Skeletal muscle tissue permeabilized in assay buffer (see Buffer Composition) was used for the spectrophotometric determination of complexes I, II+III, and IV as described [3-5]. The residual activity in presence of 2 µmol/l rotenone or 1 µmol/l antymicin A was subtracted from the total activity of each complex to insure specificity.

Mitochondria isolation and H^+-ATP synthase activity.

36h after transfection, mitochondria were isolated from myotubes using a Potter-Elvehjem homogenizer and the Mitochondria Isolation Kit (Sigma-Aldrich). Mitochondria resuspended in assay buffer (see Buffer Composition) were used for the determination of the hydrolase activity of the enzyme [3, 4]. Inhibition of the H^+-ATP synthase activity was accomplished by the addition of 30 µmol/l oligomycin.

Glucose uptake assay. Uptake of the non-metabolized analog 2-deoxyglucose (final concentration 0.01 mmol/l) was measured in triplicate over 10 minutes at room temperature [6]. An aliquot of the suspension was removed for protein analysis. The uptake of L-glucose is used to correct each sample for the contribution of diffusion. When indicated, 100 nmol/l insulin was added for 60 min at 37°C before assay.

Lactate determination. 24h after transfection the culture medium was replaced with fresh medium supplemented with 0.5% serum. Aliquots of the medium were collected at 12 h and the initial rate of lactate production determined from the concentration of

lactate appearing in the medium [1] using a YSI 2300 STAT Plus dual glucose/lactate analyzer.

Non-esterified fatty acid (NEFA) oxidation.

Cells were incubated in serum-free media containing [9,10-^{3}H] palmitic acid (0.2 μCi, final concentration = 20 μmol/l) in a 95% O2:5% CO_2 incubator at 37°C for 3h. After incubation, an aliquot (100 μl) of the culture medium was placed over an ion-exchange resin and the column washed with water. Intact NEFA (charged state) was retained by the resin, whereas the oxidized portion of NEFA passed freely through the column. All results are adjusted for total cellular protein content determined by the method of Bradford.

Determination of Glutathione, α-KG, NEFA and NAD/NADH. The skeletal muscle GSH and GSSG concentrations were determined as previously described [3]. Myotubes permeabilized with 1% Triton X-100 and resuspended in assay buffer (see Buffer Composition) were used for the spectrophotometric determination of α-KG. The free fatty acids assay kit (Sigma-Aldrich) and NAD/NADH Quantitation kit (Sigma-Aldrich) were employed to measure the NEFA content of the cytosolic fraction and the variation in NAD/NADH in total extracts of myotube cultures, respectively.

Determination of myokine secretion.

The RayBio C-Series Human Cytokine Antibody Array C3 (RayBiotech) was used for the semi-quantitative detection of 42 human proteins in cell culture media. Specific Human TNF-alpha Quantikine HS ELISA assay (R&D system) was used to confirm the data and quantify TNF-alpha levels in myotube media.

Buffer composition.

Extraction buffer: Tris HCl 20 mmol/l pH 7.4; Triton X-100 1%; NP-40 1%; PMSF 200 mol/l; leupeptin 1 mol/l; Aprotinin 10 g/ml; NaF 100 mmol/l; NaPP 40 mmol/l.

Respiratory chain complex activity assay buffer: Tris HCl 20 mmol/l pH 7.4; Triton X-100 0.1%; NP-40 0.25%; PMSF 200 mol/l; leupeptin 1 mol/l; Aprotinin 10 g/ml; NaF 100 mmol/l; NaPP 40 mmol/l. Detailed protocols and buffers in [5].

ATPase activity assay buffer: Tris HCL 20mmol/l pH 8; 5 mg/mL BSA; 20mmol/l MgCl2; 50mmol/l KCl; 5 µmol/l FCCP; 5 µmol/l Antimycin A; 10 mmol/l phosphoenolpyruvate; 2.5 mmol/l ATP; 4 µmol substrate/min Lactate dehydrogenase; 4 µmol substrate/min Pyruvate kinase; 1mmol/l NADH.

Alpha-ketoglutarate assay buffer: 0.1 mol/l phosphate buffer pH 7.5; 1.15 mol/l L-Alanine; 8 mmol/l NADH; 250 µmol substrate/min/ml LDH; 0.2 µmol substrate/min/ml GPT.

Proteomics, immunoblot and immunoprecipitation analysis:

Protein Digestion and TMT Labeling. Mitochondria enriched samples from 3 nO-nT2, 3 O-nT2D and 3 O-T2D hSMC were lysed in a buffer composed of 75mmol/l NaCl (Sigma-Aldrich), 3% sodium dodecyl sulfate (Sigma-Aldrich), 1mmol/l sodium fluoride (Sigma-Aldrich), 1mmol/l beta-glycerophosphate (Sigma-Aldrich), 1mmol/l sodium orthovanadate (Sigma-Aldrich), 10mmol/l sodium pyrophosphate (Sigma-Aldrich), 1mmol/l phenylmethylsulfonyl fluoride (Sigma-Aldrich) and 1X Complete mini EDTA free protease inhibitors (Roche, Basel, Switzerland) in 50mmol/l HEPES (Sigma-Aldrich), pH 8.5 [7]. Insoluble debris was pelleted by centrifugation at 14000 RPM for

5 minutes. Proteins were reduced and alkylated as previously described [8]. Proteins were precipitated with TCA then re-solubilized in 1 mol/l urea (Thermo Fisher Scientific) in 50 mmol/l HEPES, pH 8.5. Proteins were digested in a two-step process; 3 μg of LysC (Wako) was added to each sample and then incubated overnight at room temperature. Next, 3 μg of trypsin was added and samples were digested for 6h at 37°C. Digestion was quenched with trifluoroacetic acid (Thermo Fisher Scientific) (TFA) then desalted with C18 Sep-Paks (Waters, Milford, MA, USA) as previously described [9].

Samples were labeled with 10-plex TMT reagents (Thermo Fisher Scientific) (4,5) as previously described [10]. TMT reagents were solubilized in dry acetonitrile (Sigma-Aldrich) at 20 μg/μl. Peptides were re-suspended in 30% dry acetonitrile in 200 mmol/l HEPES, pH 8.5 and 7 μl of the appropriate TMT reagent was added to each sample. Labeling was conducted for 1h at room temperature and was quenched by addition of 8 μL of 5% hydroxylamine (Sigma-Aldrich), which was allowed to react for 15 minutes. Samples were then acidified by addition of 50 μL of 1% TFA and pooled. The pooled sample was desalted with C18 Sep-Paks as described above.

Basic pH Reverse-Phase Liquid Chromatography Fractionation. Fractionation was carried out by basic pH reverse-phase liquid chromatography [11] with fraction combining as previously described [9]. Briefly, samples were solubilized in 5% formic acid in 5% acetonitrile and separated on a 4.6 mm x 250 mm C28 column (Thermo Fisher Scientific) on an Ultimate 3000 HPLC fitted with an auto sampler, fraction collector, degasser and variable wavelength detector. Separation was performed over a 22% to 35%, 60-minute linear gradient of acetonitrile in 10 mmol/l ammonium bicarbonate (Thermo Fisher Scientific) at a flow rate of 0.5 ml/min. The resultant 96

fractions were combined as previously described [9]. Fractions were dried and re-suspended in 5% formic acid / 5% acetonitrile and analyzed by LC-MS2/MS3 for identification and quantitation.

LC-MS2/MS3 Protein Identification and Quantitation. LC-MS2/MS3 experiments were conducted on an Orbitrap Fusion (Thermo Fisher Scientific) with an in-line Easy-nLC 1000 (Thermo Fisher Scientific). Home-pulled, home-packed columns (100 μm ID x 30 cm, 360 μOD) were used for analysis. Analytical columns were triple-packed with 5 μm C4 resin, 3 μm C18 resin and 1.8 μm C18 resin (Sepax Technologies, Newark, DE, USA) to lengths of 0.5cm, 0.5cm and 30cm respectively. Samples were loaded on the column at 500 bar and eluted with a linear gradient of 11% to 30% acetonitrile in 0.125% formic acid over 165 minutes at a flow rate of 300 nl/minute with the column heated to 60°C. Nano-electrospray ionization was achieved by applying 2000V through a stainless steel T-junction at the inlet of the analytical column.

The Orbitrap Fusion was run in data-dependent mode, where a survey scan was collected over 500-1200 m/z at a resolution of 120000 in the Orbitrap. Automatic gain control (AGC) was set to 5 $x10^5$ for the survey scan, with a maximum ion injection time of 100 ms. The S-lens RF was set to 60 and centroided data were collected. For subsequent MS2/MS3 analysis, top speed mode was enabled to select the most abundant ions for analysis in a 5 second cycle.

For MS2/MS3 analysis, the decision tree option was used, with charge state and m/z range as qualifiers. Ions with a +2 charge state were analyzed from the m/z range of 600-1200, and +3/+4 ions were selected from the m/z range of 500-1200. An ion intensity trigger threshold of 5 x 10^3 was used. MS2 spectra were obtained with quadrupole isolation with a 0.5 Th window and fragmented with collision induced

dissociation using a normalized collision energy of 30%. Fragment ions were detected and centroided data collected in the linear ion trap using rapid scan rate with an AGC target of 1 x 10^4, maximum ion injection time of 35 ms.

MS3 analysis was conducted using the synchronous precursor selection (SPS) option to maximize TMT quantitation sensitivity [12]. For SPS, a maximum of 10 MS2 precursors was specified, which were simultaneously isolated and fragmented for MS3 quantitation. Higher-energy collisional dissociation was used as fragmentation for MS3, with a normalized collision energy of 50%. Resultant fragments were detected in the Orbitrap with a resolution of 60000 and a low mass cut-off of 110 m/z. AGC for MS3 spectra was set to 5x10^4 with a maximum ion injection time of 250 ms. MS2 ions from a range of 40 m/z below and 15m/z above the precursor m/z were excluded by SPS. Centroided data were collected for all MS3 scans.

Proteomic Data Processing and Analysis. Resultant data files were processed using Proteome Discoverer 2.1 (Thermo Fisher Scientific). MS2 data were queried against the Uniprot Human database using the Sequest algorithm [13]. A decoy search was also conducted with sequences in reversed order [14-16]. For MS1 spectra, a mass tolerance of 50ppm was specified and for MS2 spectra a 0.6 Da tolerance was used. Static modifications included TMT 10-plex reagents on lysine and peptide n-termini (+229.162932 Da) and carbamidomethylation of cysteines (+57.02146 Da). Variable oxidation of methionines (+15.99492 Da) was also included in the search parameters. Data were filtered to a 1% peptide and protein level false discovery rate using the target-decoy strategy [14].

Reporter ion intensities from TMT reagents were extracted from MS3 spectra for quantitative analysis, and signal to noise values were used for quantitation. Spectra

were used if the average signal to noise was greater than 10 across samples and if isolation interference was less than 25%. Protein level quantitation values were calculated by summing signal to noise values for all peptides per protein meeting the specified filters. Data were normalized in a two-step process, whereby they were first normalized to the mean for each protein. To account for variation in the amount of protein labeled, values were then normalized to the median of the entire dataset. Final values are reported as normalized summed signal to noise per protein per sample. After ANOVA and q-test analysis all data met the assumptions of the statistical approach.

Immunoprecipitation Assays. Protein from cell lysates (400 μg) was incubated with 12 μg of the indicated antibody bound to EZ View Red Protein G Affinity Gel at 4°C as previously described [2]. IP lysis buffer: 50 mmol/l Tris-HCl, pH 6.0, 150 mmol/l NaCl, 0.5% Nonidet P40, complete EDTA-free protease inhibitor cocktail (Roche), and phosphatase inhibitor cocktail (Sigma-Aldrich).

Western Blot antibodies and methodology. Proteins were size and charge fractionated by SDS-PAGE and then transferred onto nitrocellulose membranes. Protein transfer was accomplished using a Trans-Blot Cell (Bio-Rad, Hercules, CA, USA) with a constant voltage of 100 V during 35 minutes at 4ºC. The primary monoclonal antibodies developed in our lab, validated and used in this study were: HSP60 (1:5,000); anti-β-F1-ATPase (clone 11/21-7 A8; 1:20,000); anti-GAPDH (1:20,000) and the monoclonal antibody specifically recognizing the human IF1 protein (clone 14/2-1 G1; 1:200) [3]. Other previously validated antibodies were: anti-complex II subunit SDH-B (1:1000) from Life Technologies (Carlsbad, CA, USA); anti-Complex III subunit Core 2 (1:1,000) and anti-complex IV subunit COXI (1:1,000) from Abcam (Thermo Fisher

Scientific); anti-complex I subunit NDUF-9 (1:1,000); anti-SOD2 (1:5,000); anti-catalase (1:1000); anti-MNF-1 (1:1000); anti-MNF-2 (1:1000); anti-DRP1 (1:1000) and anti-OPA1 (1:1000) from Cell Signaling (Danvers, MA, USA); the pan-specific monoclonal phospho-Serine antibody (1:250) from Sigma-Aldrich (St. Louis, MO, USA). Fluorescently labeled secondary goat anti-rabbit and rabbit anti-mouse antibodies (1:5.000) were used for detection using a LiCor Odyssey CxLsystem. Quantification of the immunoreactive bands (arbitrary units) was accomplished using the Licor Image Studio analysis software (v.3.1.4). The expression of the house-keeping proteins HSP60 and GAPDH were used to normalized the blotting results.

Hierarchical clustering analyses. We used the Cluster Program at http://ep.ebi.ac.uk/EP/EPCLUST using the Euclidean distances and average linkage method (Weighted Group Average, WPGMA). Protein expression scores are shown normalized to the mean relative expression level in samples, from healthy subjects according to a color scale (below panels): red indicates high; green, low expression. The dendogram (to the right of the matrix) represents overall similarities in expression profiles. For the expression profiles of metabolic markers data were reformatted by calculating the log(2) of the expression level in each sample relative to the mean expression level in nO-nT2D subjects.

ESM text: Results

Obesity and type 2 diabetes induce perturbations in skeletal muscle mitochondria. Mitochondria are known as a key regulator of reactive oxygen species (ROS) production. Interestingly, type 2 diabetes subjects presented significantly higher levels of the mitochondrial redox sensor superoxide dismutase-2 (SOD2) in comparison to healthy subjects (Fig. 1c and ESM Fig. 1). The SOD2/HSP60 ratio inversely correlated with patient age, suggesting that muscle cells gradually lose the potential to handle ROS with aging (ESM Fig. 2). Consistent with this behavior, the red/ox glutathione ratio (GSH/GSSG) in skeletal muscle decreased with age in both O-T2D and nO-T2D groups (80% and 77% respectively) and GSH levels correlated inversely with FG concentration (r^2=0.12; p=0.05; ESM Fig 2).

To investigate a possible impairment of mitochondrial respiratory chain in obesity and type 2 diabetes, we analyzed the expression of subunits from complexes I, II, III and IV of the mitochondrial electron transport chain (ETC). The results show that neither obesity nor type 2 diabetes significantly affected the expression of complexes II and IV, although there is a slight downregulation of complex I in diabetic subjects and of complex III in O-nT2D compared to nO-nT2D (Fig. 1c and ESM Fig. 1).

ESM text: References

[1] Formentini L, Sanchez-Arago M, Sanchez-Cenizo L, Cuezva JM (2012) The mitochondrial ATPase inhibitory factor 1 triggers a ROS-mediated retrograde prosurvival and proliferative response. Mol Cell 45: 731-742

[2] Garcia-Bermudez J, Sanchez-Arago M, Soldevilla B, Del Arco A, Nuevo-Tapioles C, Cuezva JM (2015) PKA Phosphorylates the ATPase Inhibitory Factor 1 and Inactivates Its Capacity to Bind and Inhibit the Mitochondrial H(+)-ATP Synthase. Cell Rep 12: 2143-2155

[3] Formentini L, Pereira MP, Sanchez-Cenizo L, et al. (2014) In vivo inhibition of the mitochondrial H+-ATP synthase in neurons promotes metabolic preconditioning. EMBO J 33: 762-778

[4] Santacatterina F, Sanchez-Cenizo L, Formentini L, et al. (2016) Down-regulation of oxidative phosphorylation in the liver by expression of the ATPase inhibitory factor 1 induces a tumor-promoter metabolic state. Oncotarget 7: 490-508

[5] Barrientos A, Fontanesi F, Diaz F (2009) Evaluation of the mitochondrial respiratory chain and oxidative phosphorylation system using polarography and spectrophotometric enzyme assays. Curr Protoc Hum Genet Chapter 19: Unit19 13

[6] Ciaraldi TP, Abrams L, Nikoulina S, Mudaliar S, Henry RR (1995) Glucose transport in cultured human skeletal muscle cells. Regulation by insulin and glucose in nondiabetic and non-insulin-dependent diabetes mellitus subjects. J Clin Invest 96: 2820-2827

[7] Villen J, Gygi SP (2008) The SCX/IMAC enrichment approach for global phosphorylation analysis by mass spectrometry. Nat Protoc 3: 1630-1638

[8] Haas W, Faherty BK, Gerber SA, et al. (2006) Optimization and use of peptide mass measurement accuracy in shotgun proteomics. Mol Cell Proteomics 5: 1326-1337

[9] Tolonen AC, Haas W (2014) Quantitative proteomics using reductive dimethylation for stable isotope labeling. J Vis Exp

[10] Ting L, Rad R, Gygi SP, Haas W (2011) MS3 eliminates ratio distortion in isobaric multiplexed quantitative proteomics. Nat Methods 8: 937-940

[11] Wang Y, Yang F, Gritsenko MA, et al. (2011) Reversed-phase chromatography with multiple fraction concatenation strategy for proteome profiling of human MCF10A cells. Proteomics 11: 2019-2026

[12] McAlister GC, Nusinow DP, Jedrychowski MP, et al. (2014) MultiNotch MS3 enables accurate, sensitive, and multiplexed detection of differential expression across cancer cell line proteomes. Anal Chem 86: 7150-7158

[13] Eng JK, McCormack AL, Yates JR (1994) An approach to correlate tandem mass spectral data of peptides with amino acid sequences in a protein database. J Am Soc Mass Spectrom 5: 976-989

[14] Elias JE, Gygi SP (2007) Target-decoy search strategy for increased confidence in large-scale protein identifications by mass spectrometry. Nat Methods 4: 207-214

[15] Elias JE, Haas W, Faherty BK, Gygi SP (2005) Comparative evaluation of mass spectrometry platforms used in large-scale proteomics investigations. Nat Methods 2: 667-675

[16] Peng J, Elias JE, Thoreen CC, Licklider LJ, Gygi SP (2003) Evaluation of multidimensional chromatography coupled with tandem mass spectrometry (LC/LC-MS/MS) for large-scale protein analysis: the yeast proteome. J Proteome Res 2: 43-50

ESM Figures

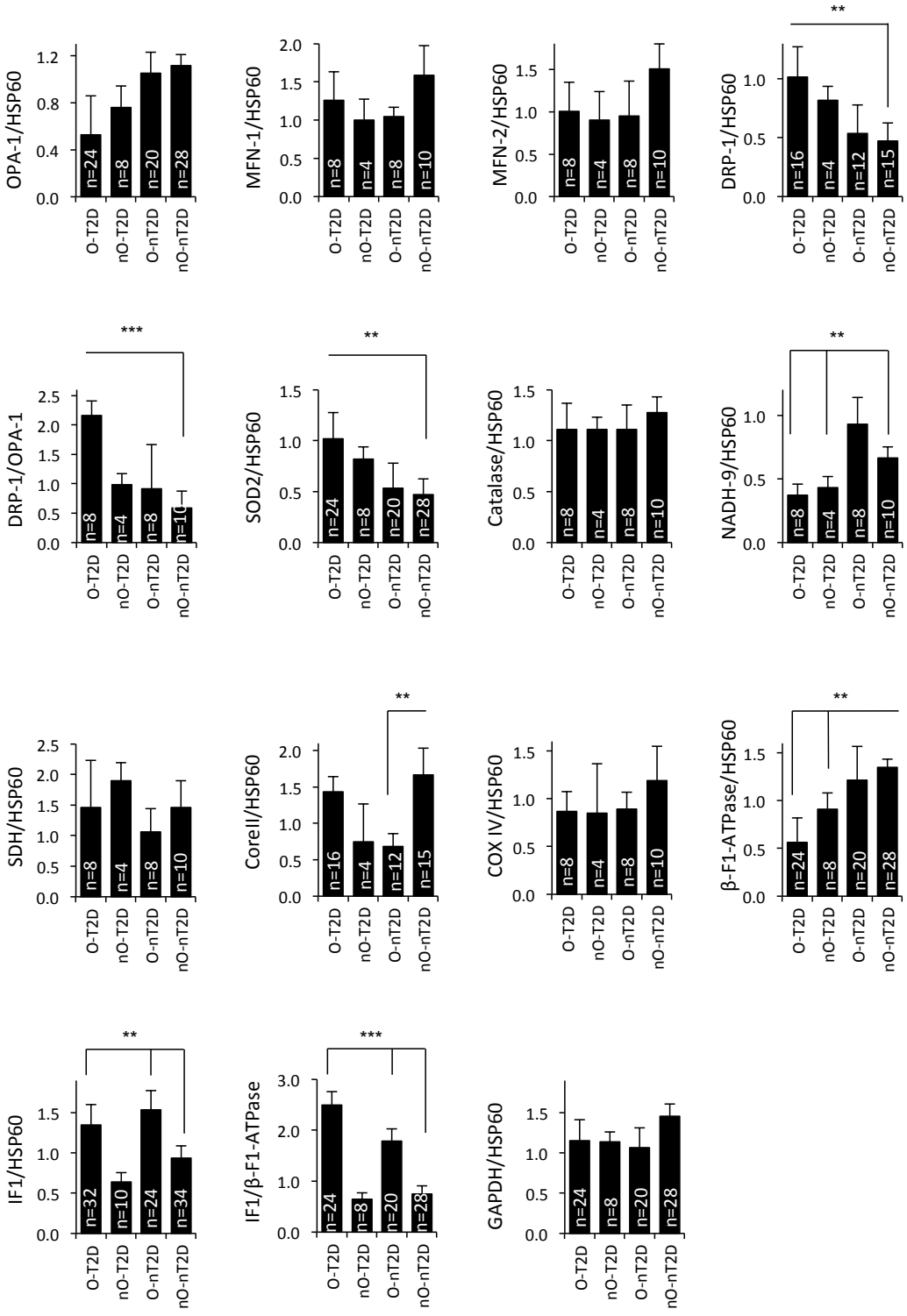

ESM Fig. 1

Histograms show the quantification of the blots presented in Fig. 1c. The n indicates the number of subjects analysed. **p*<0.05, ***p*<0.01, ****p*<0.001 by ANOVA multiple comparisons.

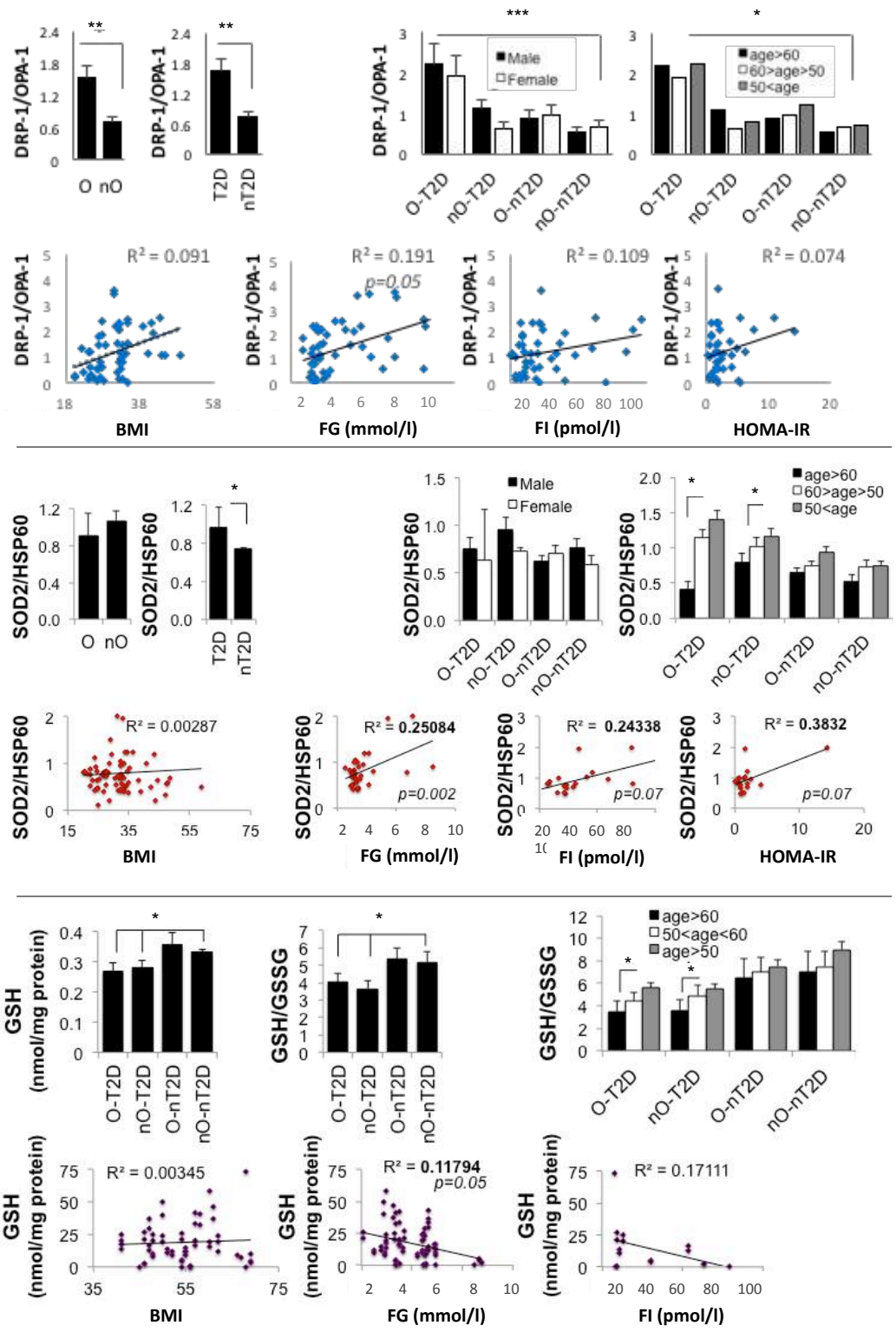

ESM Fig. 2

Top of each panel- effects of obesity, type 2 diabetes, gender and age on the expression of DRP-1/OPA-1 (upper panel), SOD2/HSP60 (central panel) and GSH/GSSG (lower panel) ratio in skeletal muscle biopsies. Bottom of each panel- correlations between indicated proteins and BMI, FG, FI and HOMA-IR. Bars are the mean ± SEM of at least 47 subjects. *p<0.05, **p<0.01, ***p<0.001 by ANOVA multiple comparisons and Student's t test.

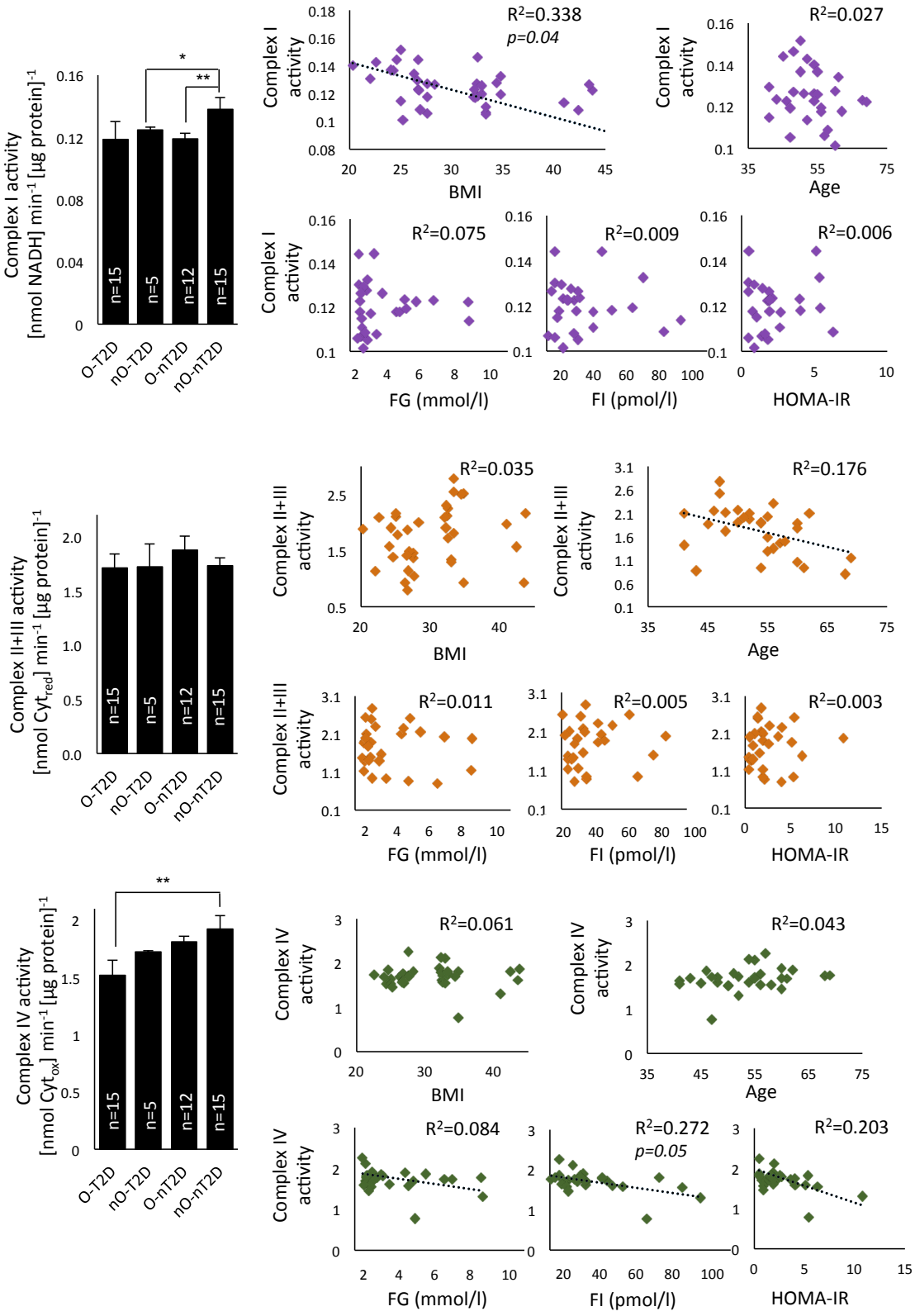

ESM Fig. 3

Correlations between mitochondrial activities of complex I (upper panel), II+III (central panel), IV (lower panel) and BMI, Age, FG, FI and HOMA-IR. Bars are the mean ± SEM of 47 subjects. **p<0.01, ***p<0.001 by ANOVA multiple comparisons.

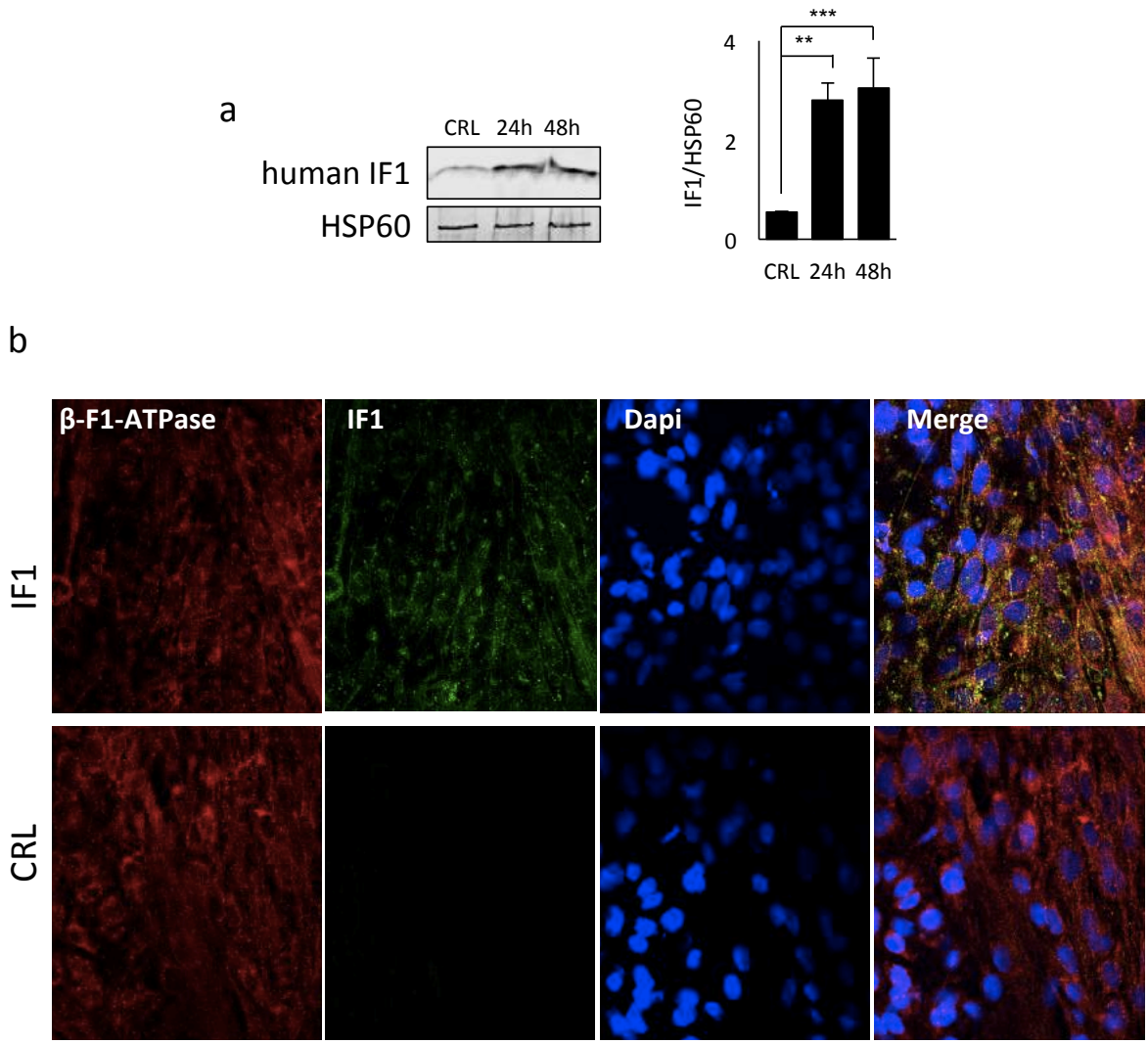

ESM Fig. 4

(**a**) Representative blots of the expression of HSP60 and IF1 after 24-h and 48-h transfection in hSMC from nO-nT2D subjects. Bars are the mean ± SEM of 3 experiments. **p<0.01, ***p<0.001 by Student's t test. (**b**) Inmunofluorescence of β-F1-ATPase (red), IF1 (green) and nuclei (Dapi, blue) in L6 cells transfected with IF1 (IF1) or control (CRL) plasmids.

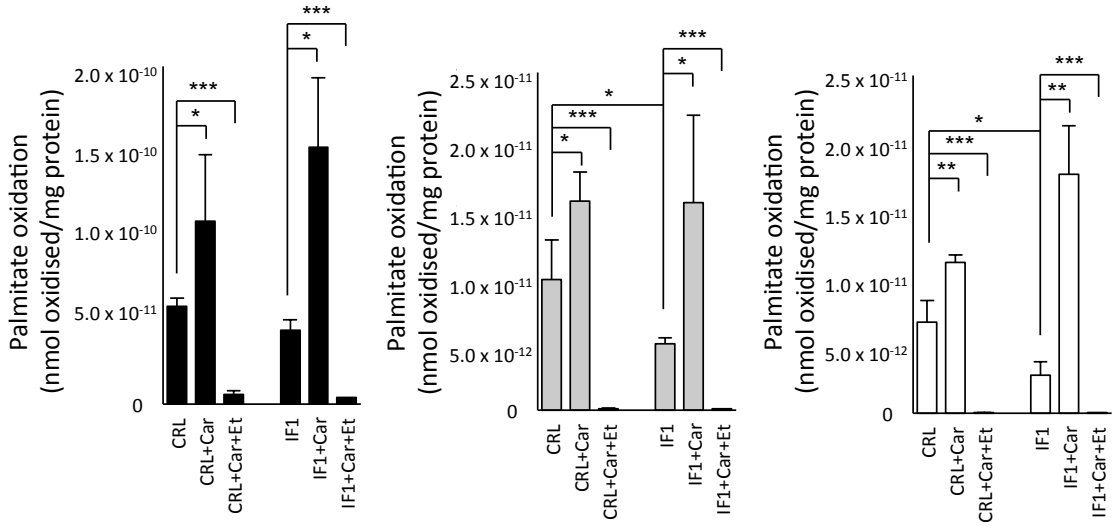

ESM Fig. 5

Palmitate oxidation in hSMC derived from 3 healthy (Non-obese, black bars), 3 obese (O, stripped bars) and 3 type 2 diabetes (O-T2D, closed bars) subjects. The effect of 36 h overexpression of IF1 (+IF1), 3-h treatment with 1mmol/l carnitine (+Car) or 100μmol/l etomoxir (+Et) are shown. Bars are the mean ± SEM. *p<0.05, **p<0.01, ***p<0.001 by ANOVA multiple comparisons.

1	POS	POS	NEG	NEG	ENA-78	G-CSF	GM-CSF	GRO	GRO alpha	I-309	IL-1 alpha	IL-1 beta
2	POS	POS	NEG	NEG	ENA-78	G-CSF	GM-CSF	GRO	GRO alpha	I-309	IL-1 alpha	IL-1 beta
3	IL-2	IL-3	IL-4	IL-5	IL-6	IL-7	IL-8	IL-10	IL-12 p40/70	IL-13	IL-15	IFN gamma
4	IL-2	IL-3	IL-4	IL-5	IL-6	IL-7	IL-8	IL-10	IL-12 p40/70	IL-13	IL-15	IFN gamma
5	MCP-1	MCP-2	MCP-3	M-CSF	MDC	MIG	MIP-1 delta	RANTES	SCF	SDF-1	TARC	TGF beta 1
6	MCP-1	MCP-2	MCP-3	M-CSF	MDC	MIG	MIP-1 delta	RANTES	SCF	SDF-1	TARC	TGF beta 1
7	TNF alpha	TNF beta	EGF	IGF-1	ANG	OSM	THPO	VEGF	PDGF BB	Leptin	NEG	POS
8	TNF alpha	TNF beta	EGF	IGF-1	ANG	OSM	THPO	VEGF	PDGF BB	Leptin	NEG	POS

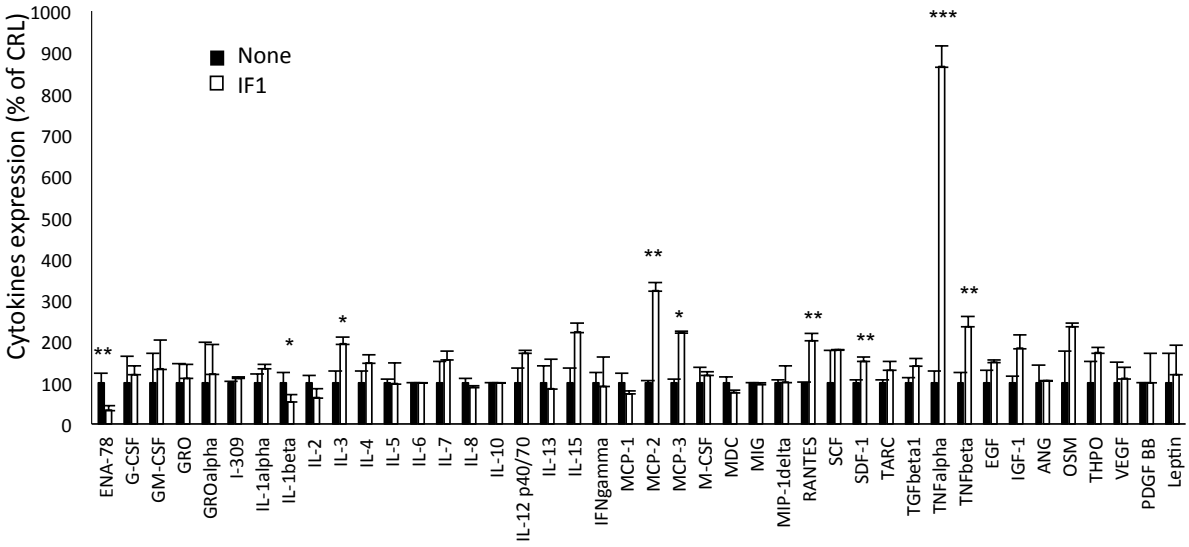

ESM Fig. 6

The RayBio® C-Series Human Cytokine Antibody Array C3 (RayBiotech) in Fig. 4a. POS: Positive Control Spot; NEG: Negative Control Spot.

The chart shows the comparison between secretomes of control (CRL) and IF1 overexpressing (IF1) myotubes from O-T2D individuals. Bars are mean ± SEM of 3 independent experiments. *p<0.05, **p<0.01, ***p<0.001 by ANOVA multiple comparisons.